
THE SPATIAL DISTRIBUTION OF Ca^{2+} SIGNALS INDUCED BY Ca^{2+} ENTRY THROUGH LVA Ca^{2+} CHANNELS IN P12 LD THALAMIC NEURONS

A.N. TARASENKO, D. ISAEV, A. YEREMIN,
A. IVANOV, V. LUHOVSKY, A. PALAHINA, E. KADOCHNIKOV

Bohomolets Institute of Physiology, Kyiv, Ukraine
tar@biph.kiev.ua



July 1992 was the start point for Dr. A. Tarasenko for investigation of the LVA Ca^{2+} channel properties on rat brain slice preparations. The first demonstration of the LVA Ca^{2+} channels activity in the rat laterodorsal (LD) thalamic neurons *in situ* was made at the beginning of 1994. During the following year we confirmed that LVA Ca^{2+} channels expressed by LD thalamic during the first two weeks postnatal were sensitive to nifedipine with $K_d = 2.6 \mu\text{M}$. Next two years, 1995-1996, we investigated the developmental time course of LVA Ca^{2+} channels during the first three postnatal weeks in LD thalamic neurons, visual and somatosensory cortical neurons. The data suggested the existence of two LVA Ca^{2+} channels subtypes in one particular neuron with different kinetic properties. The channels were inactivated either

fast (~ 24 ms) (LVAf) and were nifedipine sensitive or slow (~ 65 ms) (LVAs) without sensitivity to nifedipine. They had different developmental time course. LVAs Ca^{2+} channels appeared at the end of the second postnatal week, while LVAf ones were presented over the all tested period. The first publication named as "Two types of LVA Ca^{2+} channels in neurons of rat laterodorsal thalamic nucleus" appeared in 1997 in *J. Physiology*. The second was named as "Developmental changes in the expression of low-voltage-activated Ca^{2+} channels in rat visual cortical neurons" and also published in *J. Physiology* in June 1998. When the first pictures of the LD thalamic neurons *in situ* (courtesy to A. Ivanov) and isolated neurons were made, it was clear that the neurons have dramatically different dendritic tree geometry. Analysis of the surface area of P12 tested neurons and the amount of the charge transferred during LVA Ca^{2+} channels activation suggested a correlation such as the less dendritic tree branches were developed, the smaller amount of the charge was transferred. The conclusion was that the number of LVA Ca^{2+} channels distributed over the same surface area in different tree geometry neurons may significantly differ. The first attempt to map active LVA Ca^{2+} channels was made in Much-June 2003. V. Lugovskoy in the laboratory of Prof. Bolsover (UCL, London) visualized the calcium concentration increase induced by Ca^{2+} entry through LVAf Ca^{2+} channels in isolated P12 LD thalamic neurons. The LVAf Ca^{2+} channels activation and Fluo-3 dye loading were made using patch pipette in the whole-cell configuration. CCD camera was used to control Ca^{2+} signal distribution induced by Ca^{2+} entry. We started developing the electrophysiological protocol allowing activation of a single LVAf Ca^{2+} channels at 2mM Ca^{2+} in the extracellular solution and without zeroing the resting membrane potential (RMP). The measurement of the charge transferred via small patched surface area (from ~ 10 to $\sim 30 \mu\text{m}^2$) during LVAf Ca^{2+} channels activity suggested that these channels are grouped in multichannel domains at least over the somatic membrane.

The photo shows a student of P.G. Kostyuk, A.N. Tarasenko.

Methodological aspects of Ca²⁺ entry visualization

Entry of Ca²⁺ through LVA Ca²⁺ channels is an important event for maintenance of the intraneuronal communication and neuronal excitability control. However, what is the result of this entry in each particular neuron? This question requires investigation in two aspects. First, one should image the LVA Ca²⁺ channels distribution in real 3-dimensional (3D) neuronal structure. Second, the amount of charge transfer via an active single channel should be estimated in physiological conditions. Up to date, both two aspects are not clear. Moreover, expression of either one or two LVA Ca²⁺ channels subtypes simultaneously in one particular laterodorsal (LD) thalamic neuron depends on the postnatal (P) developmental stage (Tarasenko et al., 1997). We have found that neurons at the second postnatal day, P2 neurons, P7 and P12 ones (unpublished data) express only fast-inactivating nifedipine-sensitive LVA Ca²⁺ channels (LVA_f). In contrast, P14 and P17 LD thalamic neurons can have both subtypes simultaneously (Tarasenko et al., 1997). Thus, we have chosen P12 LD thalamic neurons since in those neurons nifedipine (100 μM) completely blocks the Ca²⁺ entry (Tarasenko et al., 1997).

Total internal reflection fluorescent (TIRF) microscope with a CCD camera attached is an accurate instrument to excite and image fluorescence within a thin (~100-200 nm) layer next to the coverglass (Demuro and Parker, 2004). Indeed, authors observed an activity of >100 N-type Ca²⁺ channels expressed in oocyte. In contrast to TIRF, a wide-field microscope does not have a focal plane restriction. It was successfully used to visualize Ca²⁺ entry through plasma membrane cation channels (Zou et al., 1999) randomly distributed over smooth muscle cells membrane. Charge entry induced by caffeine was controlled in the whole-cell configuration. We also used a wide-field microscope to accumulate the fluorescent light. The charge entry through active LVA_f Ca²⁺ channels was controlled in the whole-cell configuration, and the results of Ca²⁺ entry was detected as an accumulated Fluo-3 fluorescence increase.

Control of the amount of charge entry through multiple LVA_f Ca²⁺ channels in whole-cell configuration

To block voltage-dependent Na²⁺ and K⁺ channels, Na⁺ was replaced with choline (Chol⁺) and tetrodotoxin (TTX, 1 μM) was added to the extracellular solution. K⁺ was replaced with Cs⁺ in intracellular solution, and tetraethylammonium (TEA, 10 mM) was added to extra- and intracellular solutions. We have previously shown that P12 LD thalamic neurons in slice preparations have a mean membrane capacitance (C_m) of 84 pF. Gentle mechanical isolation after enzyme treatment allowed us to isolate neurons with C_m varied from 7 to 45 pF. Typical light microscopy pictures show dramatic variations in the dendritic tree geometry (Fig. 1, a). In spite of the significant dendritic tree truncation, both Ca²⁺ channel

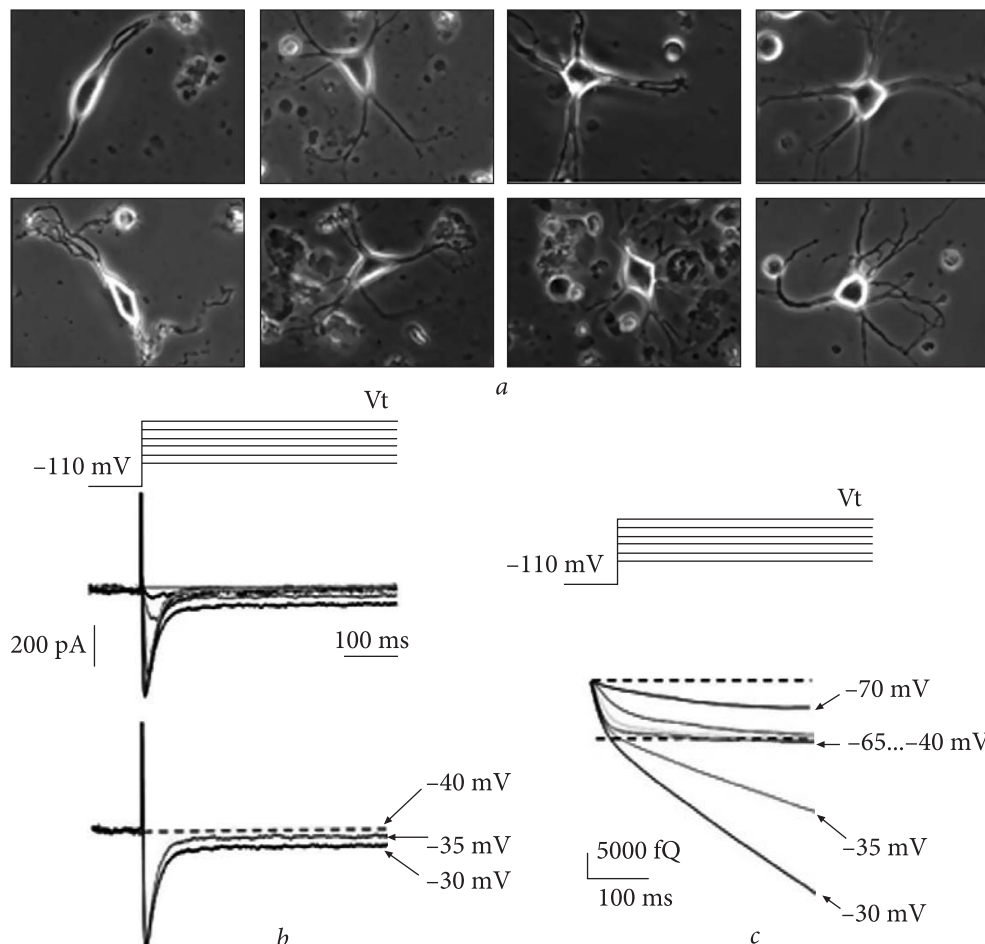


Fig. 1. Dendritic tree geometry variation and basic properties of the charge entry through whole-cell LVA Ca^{2+} channels: *a* — the most common pictures and variability within two groups of tested neurons, bi- and multipolar; *b* — typical voltage dependency of the current and charge traces induced by step depolarization

types were presented in isolated neurons. Step depolarization (V_t) from a holding potential (V_h) of -110 mV within the range from -70 to -40 mV evoked a transient LVA Ca^{2+} currents whose amplitude peaked at about -55 mV. The inactivation time constant was voltage-dependent and ranged from ~ 45 ms (at -65 mV) to 18-20 ms (at -50 mV). Sustained HVA Ca^{2+} currents appeared at V_t more positive than -40 mV (Fig. 1, *b*).

Current integration was used to estimate the amount of charge entry (Fig. 1, *c*). In each particular neuron, the charge amount had its saturation limit, and it was weakly voltage-dependent within the activation range from -65 to -45 mV. In contrast, the latency period (time from 5% to 95% of the saturation limit) was

clearly voltage-dependent. It was ranged from ~220 ms at -65 mV to ~90 ms at -50 mV. We further used this saturation limit as a passport characteristic of each tested neuron to investigate relationship between the saturation limit, or maximum of the charge amount (Q_{\max}), and the total neuronal surface area (S_{area}).

All tested neurons ($n = 45$) were subdivided into two groups. The neurons of the first group ($n = 20$) had an oval somatic shape with two dendrites emerging from opposite poles of the soma. We called these neurons as bipolar ones. Q_{\max} within this group ranged from ~1200 fC to ~6000 fC. For each tested neuron, Cm was estimated by integration of the capacitance transient induced by 10 mV step hyperpolarization. In bipolar neurons it varied from ~10 to 34 pF. As the surface area (S_{area}) increased, Q_{\max} -Cm plot approached the saturation value. The neurons from the second group had from 3 to 5 bifurcating dendrites. We called these neurons as multipolar ones. Within this group Q_{\max} varied from 5400 to 23000 fC, at the same time, Cm had about the same range from ~12 to 45 pF. Having about the same surface area, multipolar neurons had much powerful potential for charge entry than that in bipolar neurons. This strongly suggested that multipolar neurons have larger amount of the active LVA_f Ca²⁺ channels and presumably, a structurally different distribution of them. To investigate this in detail, we restricted the membrane surface area by pipette tip and measured the charge entered through active LVA_f Ca²⁺ channels in the cell-attached configuration. We expected to activate LVA_f Ca²⁺ channels by local extracellular potential changes.

Control of the amount of charge entry through LVA_f Ca²⁺ channels in cell-attached configuration

In order to have a comparable set of data, the same concentration of Ca²⁺ in extracellular solutions was used in our cell-attached recordings. We also bathed neurons with 2.5 mM K⁺ to keep their resting membrane potential (RMP) as it is. Extracellular Na⁺ was replaced with choline. As a general rule, upward current deflection was treated as a motion of cation ions from pipette into the cytosol. Thus, only Ca²⁺ or K⁺ ions may cause upward current deflection. When pipette potential (V_p) was of 0 mV, the membrane potential difference (MPD) was equal to RMP. Any other V_p was treated as a local potential referred to the RMP such as positive pipette potential increased the MPD, when negative one decreased it. In fact, holding pipette potential from +20 to +65 mV about 1 sec fully controlled the LVA_f Ca²⁺ channels availability. Once pipette potential (V_p) stepped back to the potentials from ~+10 to -15 mV, a set of transient currents was recorded. These currents had upward deflection. Their kinetic behavior, parameters of activation and inactivation curves were similar to those obtained in the whole-cell configuration. K⁺ was excluded as a charge carrier because at these V_t potentials a K⁺ current flows from the cytosol into the pipette, and the single-

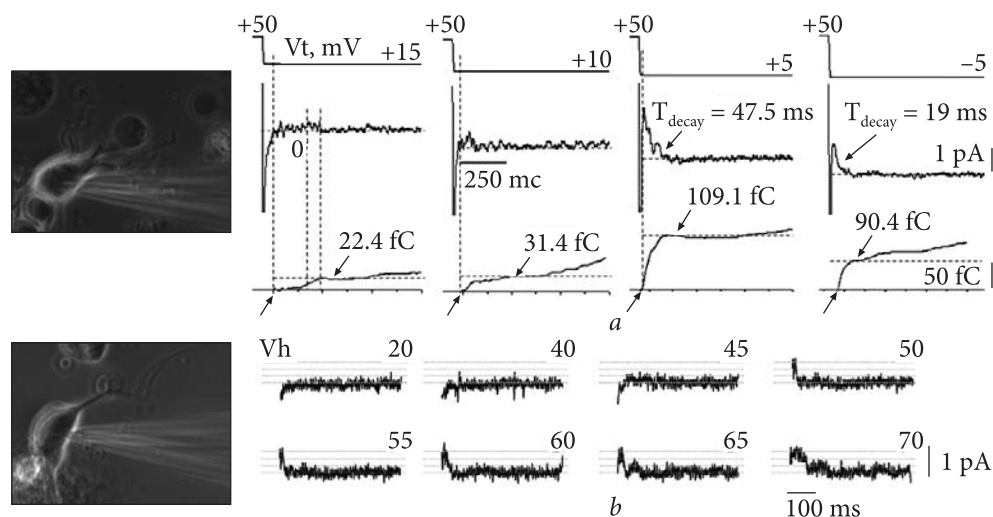


Fig. 2. Control of Ca^{2+} entry through $\text{LVA}_f \text{Ca}^{2+}$ channels in cell-attached configuration: *a* — $\text{LVA}_f \text{Ca}^{2+}$ currents as a function of V_t (indicated in Figure) in multipolar neuron. V_h is of +50 mV; *b* — $\text{LVA}_f \text{Ca}^{2+}$ currents as a function of V_h (indicated in Figure) in bipolar neuron. V_t is of +10 mV. Note that pipette tip shows the patch location

channel current will have downward deflection. Thus, the upward transient currents were associated with $\text{LVA}_f \text{Ca}^{2+}$ channels. Integration of the current resulted in charge estimation.

Fig. 2, *a* demonstrates original somatic cell-attached recordings in multipolar neuron. From patch-to-patch q_{\max} varied from ~ 60 to ~ 140 fC. However, as in the whole-cell configuration, there was no linear relationship found between q_{\max} and s_{area} . Moreover, patches with the surface area of $\sim 10 \mu\text{m}^2$ and twice larger one ($\sim 20 \mu\text{m}^2$) might have the same amount of the charge transferred. Interestingly, no $\text{LVA}_f \text{Ca}^{2+}$ channels activity was found in 9 out of 10 patches (success rate is 10 %) when patched surface area was $\sim 10 \mu\text{m}^2$. The success rate increased up to five times when s_{area} was within the range of $20\text{--}30 \mu\text{m}^2$. We further focused on the estimation of the maximum amount of charge entry through one active $\text{LVA}_f \text{Ca}^{2+}$ channel (θ_{\max}). We used Fetchan 6.0 (pClamp, Axon Instrument) as a tool for single-channel current levels investigation. We found that for multipolar neurons the number of conducting levels varied from 5 to 7. We suggested that $\text{LVA}_f \text{Ca}^{2+}$ channels in multipolar neurons are grouped in multichannel domains. Together with previous observations, the last one means that not every $10 \mu\text{m}^2$ contains a multichannel domain. Original currents as a function of V_t and corresponding charge traces for bipolar neuron is presented in Fig. 2B. For bipolar neurons, q_{\max} was significantly smaller than for multipolar ones and varied from ~ 16 to ~ 60 fC. The number of conducting levels varied from 1 to 3. This resulted in the final calculation of the θ_{\max} mean value. It was ~ 20 fC.

Ca^{2+} imaging experiments

Isolated P12 LD thalamic neurons were loaded with Fluo-3 (100 μM). They were illuminated at 490nm and two emitted light ($515 \text{ nm} < \lambda < 565\text{nm}$) images acquired, each representing accumulated light over 500 ms exposure time. A 500 ms depolarization was synchronized with the second image acquisition period, while the first one was started at the beginning of the membrane hyperpolarization, or holding potential (V_h). The images were analyzed in Lucida (Kinetic Imaging, Nottingham). Changes in the spatial intensity and ΔF signal, or total fluorescence signal increases, were calculated by subtracting the first image from the second. A special attention was paid to find a correction factors that converted images acquired at -110 and -50 mV, when $\text{LVA}_f \text{Ca}^{2+}$ channels become available for activation and activated. Nifedipine (100 μM) was used to completely block the Ca^{2+} entry via $\text{LVA}_f \text{Ca}^{2+}$ channel. This fact was controlled in voltage-clamp conditions using the whole-cell configuration. Activation of $\text{LVA}_f \text{Ca}^{2+}$ channels resulted in clearly detectable ΔF signal in both somatic and dendritic tree regions. This was observed in bipolar neurons (Fig. 3, *a*) and multipolar neurons (Fig. 3, *b*).

Analysis of the spatial distribution of the ΔF signal revealed two characteristic features. ΔF signal had either a diffusive appearance in the somatic body and

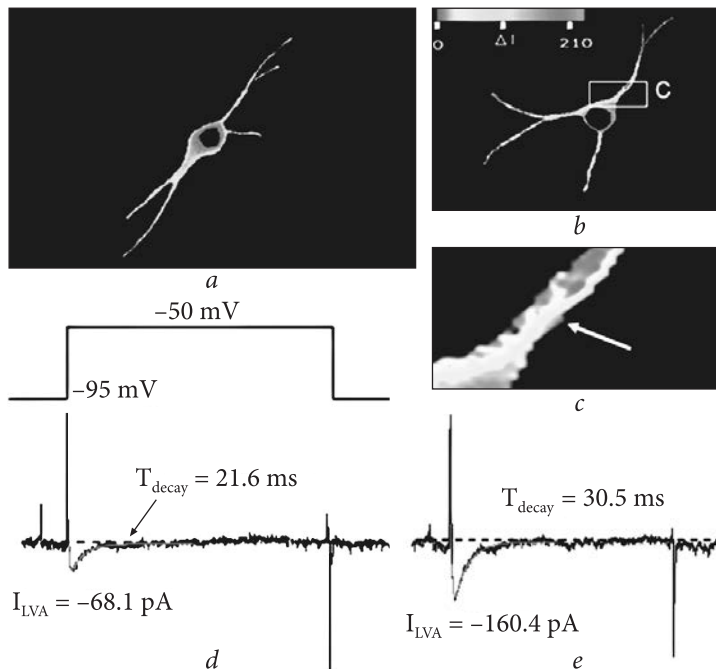


Fig. 3. Control of Ca^{2+} entry through $\text{LVA}_f \text{Ca}^{2+}$ channels in whole-cell configuration: *a* — ΔF signal induced by step depolarization in bipolar neuron; *b* — ΔF signal induced by step depolarization in multipolar neuron; *c* — spatial distribution of the "cold" (blue) and "hot" area induced by Ca^{2+} entry in multipolar neuron; *d* and *e* — original $\text{LVA}_f \text{Ca}^{2+}$ currents

dendrite tree or a well near-membrane localised patchy distribution in the form of either flashes and/or elongated sources of light and blank spaces (Fig. 3, c). When the charge amount was less than ~ 1200 fC (the amplitude of LVA_f Ca^{2+} channels was ~ 35 pA, 20 ms decay), the diffusive appearance was observed in all tested neurons. Fluorescence increases were detected in soma and dendrites regions. The use of θ_{max} (20 fC) to calculate amount of the active channels gave the value of ~ 65 . The mean Cm for bipolar neurons was ~ 20 pF or $2000 \mu m^2$. Thus, in assumption of random channel distribution, one active channel may be found over the surface area of $30 \mu m^2$ with 100% of the success rate, which agrees with our calculations described early. However, when Q_{max} was over 1200 fC at about the same S_{area} , the estimated amount of the active channels increased.

In conclusion one can say that in P12 LD thalamic multipolar neurons the LVA_f Ca^{2+} channels are grouped in multichannel domains. One domain has from 3 to 7 active LVA_f Ca^{2+} channels. The estimated surface area that contains one domain is of $\sim 60 \mu m^2$. However, spatially this domain occupies the surface area that is less than $20 \mu m^2$. Such mosaic distribution with blank spaces and channel domains presumably approaches the uniform one in bipolar neurons which exhibit small number of LVA_f Ca^{2+} channels (1-2 channels per $20 \mu m^2$) and generate whole-cell LVA_f Ca^{2+} currents with amplitude within the range of 35-60 pA. It is not yet clear at what parameters of Q_{max} and S_{area} random distribution with small number of channels transfers to a multichannel domain structure. However, there is some restriction on the expression of LVA_f Ca^{2+} channels associated with choice of neurons. Even with a large surface of the dendritic tree, bipolar neurons has no potential to express LVA_f Ca^{2+} channels in the number produced by multipolar neurons.

Acknowledgements. We thank Prof. Kostyuk for this work start in 1992 and two publications made in J.Phys. in 1997 and 1998. We also thank Prof. Bolsover from UCL, London, for the experimental design and opportunity to perform Ca^{2+} imaging experiments. The authors' work in both Kyiv and London was supported by grants from INTAS-97-32194 and the Wellcome Trust N064222 to TAN.

REFERENCES

- Demuro A, Parker I, 2004. Imaging the activity and localization of single voltage-gated Ca^{2+} channels by total internal reflection fluorescence microscopy. *Biophys. J.* 86: 3250-3259.
- Tarasenko AN, Kostyuk PG, Eremin AV, Isaev DS, 1997. Two types of low-voltage-activated Ca^{2+} channels in neurones of rat laterodorsal thalamic nucleus. *J. Physiol* 499 (Pt 1): 77-86.
- Zou H, Lifshitz LM, Tuft RA, Fogarty KE, Singer JJ, 1999. Imaging Ca^{2+} entering the cytoplasm through a single opening of a plasma membrane cation channel. *J. Gen. Physiol* 114: 575-588.
- Zou H, Lifshitz LM, Tuft RA, Fogarty KE, Singer JJ, 2004. Using total fluorescence increase (signal mass) to determine the Ca^{2+} current underlying localized Ca^{2+} events. *J. Gen. Physiol* 124: 259-272.